

A Study of the Long-Wavelength Optical Lattice Vibrations in Quaternary $\text{Al}_x\text{In}_y\text{Ga}_{1-x-y}\text{N}$ Alloys

A.I. Aljameel^{1,2,*}, H. Abu Hassan¹, S.S. Ng¹

¹ Nano-Optoelectronics Research and Technology Laboratory, School of Physics, Universiti Sains Malaysia, 11800 Minden, Penang, Malaysia

² Faculty of science, Department of Physics, Al Imam Mohammad Ibn Saud Islamic University (IMSIU)

*E-mail: abo_anas_1@yahoo.com

Received: 1 November 2012 / Accepted: 5 April 2013 / Published: 1 May 2013

Fourier transform infrared (FTIR) spectroscopy was utilized to measure the long-wavelength optical lattice vibrations of high-quality quaternary $\text{Al}_x\text{In}_{1-x-y}\text{Ga}_y\text{N}$ thin films at room temperature. With AlN as buffer layers, the $\text{Al}_x\text{In}_{1-x-y}\text{Ga}_y\text{N}$ films were grown on c-plane (0001) sapphire substrates, using the plasma-assisted molecular beam epitaxy (PA-MBE) technique with aluminium (Al) mole fraction x ranging from 0.0 to 0.2 and constant indium (In) mole fraction $y = 0.1$. The $\text{Al}_x\text{In}_{1-x-y}\text{Ga}_y\text{N}$ alloy exhibited two-mode behaviour, which includes A_1 (LO) and E_1 (TO).

Keywords: AlInGaN; FTIR; sapphire; s-polarized; p-polarized

1. INTRODUCTION

Recently, III nitride semiconductors have emerged as leading materials for the fabrication of blue-green light-emitting diodes (LEDs) and laser diodes. Alloys of GaN with InN and AlN can be prepared, covering the spectral range from red to vacuum ultraviolet (UV) (1.9 eV to 6.2 eV) [1–3]. Likewise, AlInGaN quaternary alloys have attracted significant attention due to their potential applications for UV optoelectronic devices [4–8]. Quaternary nitride alloys are important heterostructure engineering tools, because they allow the independent variation of the energy gap and lattice parameter as well as the possibility of achieving polarization-matched nitride heterostructures that are free of internal electric fields [9]. Ternary AlGaIn (UV-LEDs) have much lower efficiency than InGaIn-LEDs because of difficulties in achieving p-type conductivity with increasing Al content and the lack of efficient exciton localization, thereby making carriers very sensitive as non-recombination centres (NRCs). Therefore, using quaternary AlInGaIn alloys have been proposed to

improve UV-LEDs [10]. However, despite the rapid development in device applications, the fundamental optical properties of the AlInGaN alloys have not been well exploited. The growth condition of $\text{Al}_x\text{In}_y\text{Ga}_{1-x-y}\text{N}$ alloys is very complicated [11]. The phonon mode behaviour has not been widely investigated experimentally due to the lack of quaternary samples covering the whole composition range. Moreover, quaternary nitrides are very complex materials and cannot be explained by the usual properties of wurtzite structure.

Therefore, in the present work, we aim to investigate the fundamental optical properties of the quaternary $\text{Al}_x\text{In}_y\text{Ga}_{1-x-y}\text{N}$ samples as a function of the Al mole fraction and constant In using Fourier transform infrared (FTIR) spectroscopy measurements. The phonon modes result in quaternary samples that, to date, remain experimentally incomplete. In addition, no agreement has been made as to whether the AlInGaN phonons can be classified as having one-mode [12], two-mode [13-15], or mix-mode behaviour. Thus, the current experimental study addresses a few of the issues related to phonon modes.

2. EXPERIMENT

The samples used in this study were alloys of $\text{Al}_x\text{In}_y\text{Ga}_{1-x-y}\text{N}$ quaternary nitrides with different aluminum (Al) mole fraction x values ranging from 0.0 to 0.2 and constant indium (In) mole fraction $y = 0.1$. The samples were grown on c-plane (0001) sapphire (Al_2O_3) substrates with AlN buffer layers, using the plasma assisted molecular beam epitaxy (PA-MBE) technique. The thickness levels of the AlInGaN epilayers ranged from 0.11 μm to 0.13 μm , as measured by Filmetrics F20-VIS. Polarized IR reflectance measurements by FTIR were taken at room temperature and at an incident angle of 15° , with the aid of the Perkin-Elmer variable angle reflectance accessory. An aluminium coated mirror was employed as reference standard, with a potassium bromide (KBr) beam splitter and a mid-IR triglycine sulfate (TGS) detector. The spectra were recorded using 64 scans at a resolution of 4 cm^{-1} .

3. RESULTS AND DISCUSSION

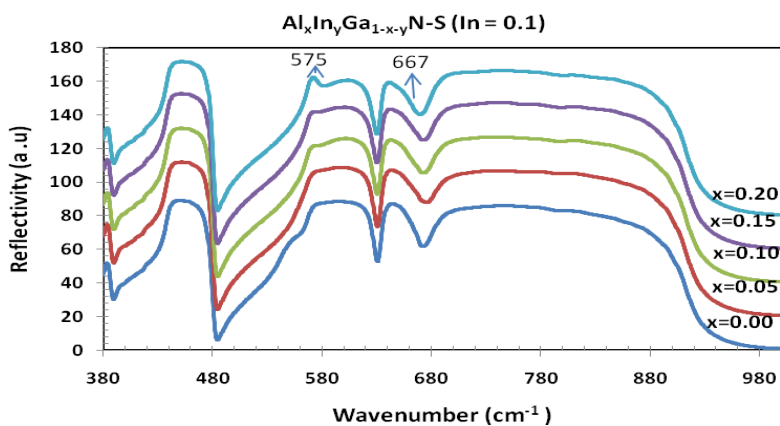


Figure 1. Room temperature FTIR of s-polarized spectra for the ternary $\text{In}_y\text{Ga}_{1-y}\text{N}$ and quaternary $\text{Al}_x\text{In}_y\text{Ga}_{1-x-y}\text{N}$ samples.

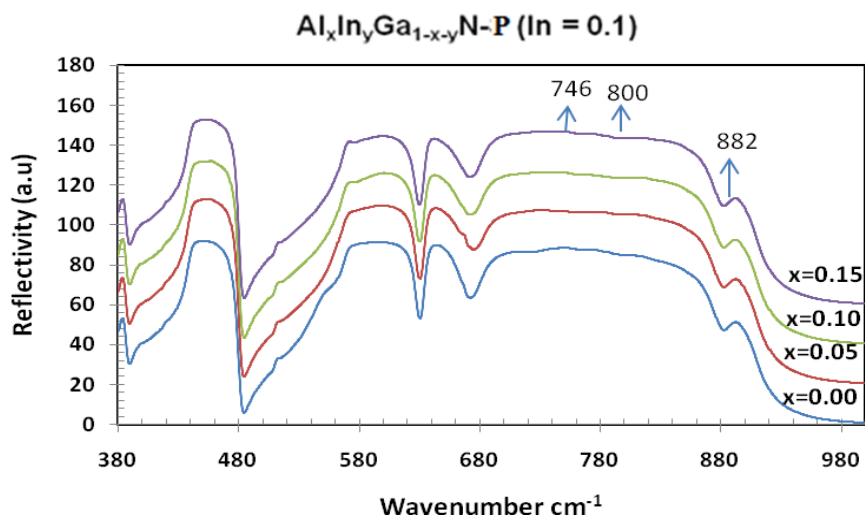


Figure 2. Room temperature FTIR of p-polarized spectra for the ternary $\text{In}_y\text{Ga}_{1-y}\text{N}$ and quaternary $\text{Al}_x\text{In}_y\text{Ga}_{1-x-y}\text{N}$ samples.

IR reflectance measurements with s- and p-polarization are performed. Under this mode, purely TO and LO phonon modes can be observed for phonon propagation direction perpendicular (\perp) and parallel (\parallel) to the crystal axis; hence, more strongly marked features can be obtained [16]. Basically, the optical phonon modes obtained from the s- and p-polarized IR reflectance measurements can be correlated to $E_1(\text{TO})$ and $A_1(\text{LO})$ modes at the centre of the Brillouin Zone (BZ), respectively [17,18]. The $E_1(\text{TO})$ mode is located at the sharp rise position of a high reflectivity feature in s-polarized reflectivity spectrum, while the $A_1(\text{LO})$ mode is located precisely at the dip position of the p-polarized reflectivity spectrum [19]. (Berreman, 1963).

Figs. 1 and 2 show the infrared reflectance measurement with s- and p- polarizations, respectively. Under these conditions, purely transverse optical $E_1(\text{TO})$ and longitudinal optical $A_1(\text{LO})$ phonon modes can be observed for the phonon propagation direction that are perpendicular and parallel to the crystal axis, respectively. Generally, it can be seen that both sets of the polarization spectra of the $\text{Al}_x\text{In}_y\text{Ga}_{1-x-y}\text{N}$ samples display almost the same patterns and are dominated by Al_2O_3 reststrahlen bands. Nevertheless, the features due to the $\text{Al}_x\text{In}_y\text{Ga}_{1-x-y}\text{N}$ thin films still can be distinguished from the pure Al_2O_3 spectra. From these two figures, both polarized reflectance spectra appear similar, except for the pronounced dip at $\sim 882 \pm 1 \text{ cm}^{-1}$ in the p-polarized spectrum and the peak in the s-polarized spectrum at $\sim 667 \pm 1 \text{ cm}^{-1}$. There are two maximum dips appeared at 484.6 ± 1 and $630.2 \pm 1 \text{ cm}^{-1}$, respectively, in the whole compositional range, which can be attributed to the sapphire substrates [20]. The other dip at $882.7 \pm 1 \text{ cm}^{-1}$ is also ascribed to the sapphire substrates because the quaternary samples are too thin at 100 nm to 130 nm. Thus, the reflectance of the sapphire modes is fairly significant in this study. Furthermore, the maximum dip at $673.9 \pm 1 \text{ cm}^{-1}$, which remained at its position in the whole compositional range, is attributed to the AlN buffer layers [21]. In Fig. 2, weak dips at $\sim 746 \pm 1$ and $800 \pm 1 \text{ cm}^{-1}$ are assigned to the $A_1(\text{LO})$ modes of the quaternary nitrides.

Regarding the $E_1(\text{TO})$ of the quaternary samples, Fig. 1 clearly shows a new peak in the quaternary samples, which was not in the ternary sample at around $585.8 \pm 1 \text{ cm}^{-1}$. The peak shifts to lower numbers at $575.5 \pm 1 \text{ cm}^{-1}$ when the Al mole fraction increases to $x = 0.20$. Similarly, another peak can be identified for the quaternary samples at $667 \pm 1 \text{ cm}^{-1}$. These two peaks represent the two modes for the $E_1(\text{TO})$ of the quaternary nitrides; their values are quite new and have not been mentioned in previous reports.

Most importantly, the present study agrees with the two-mode behaviour of quaternary nitrides. Quaternary nitrides that cover the whole range of Al and In compositions are important in studying the exact behaviour of the phonon modes. Table 1 shows the experimental optical phonon modes of our samples.

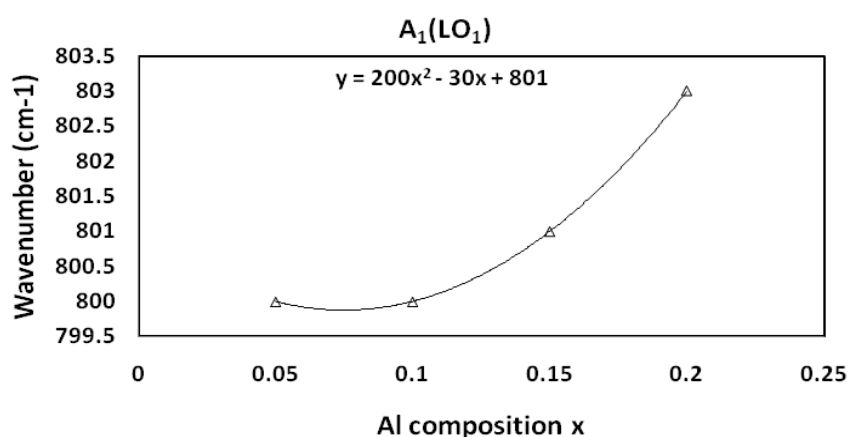


Figure 3. The $A_1(\text{LO}_1)$ optical phonon mode behaviour of $\text{Al}_x\text{In}_y\text{Ga}_{1-x-y}\text{N}$ ($0 \leq x \leq 0.2$), the solid line indicates the non-linear interpolation of the $\text{Al}_x\text{In}_y\text{Ga}_{1-x-y}\text{N}$ $A_1(\text{LO}_1)$ data

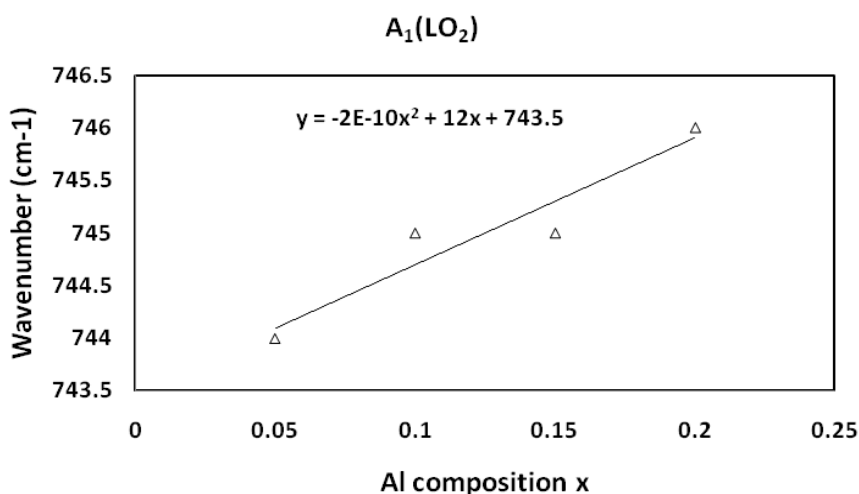


Figure 4. The $A_1(\text{LO}_2)$ optical phonon mode behaviour of $\text{Al}_x\text{In}_y\text{Ga}_{1-x-y}\text{N}$ ($0 \leq x \leq 0.2$), the solid line represents the non-linear interpolation of the $\text{Al}_x\text{In}_y\text{Ga}_{1-x-y}\text{N}$ $A_1(\text{LO}_2)$ data.

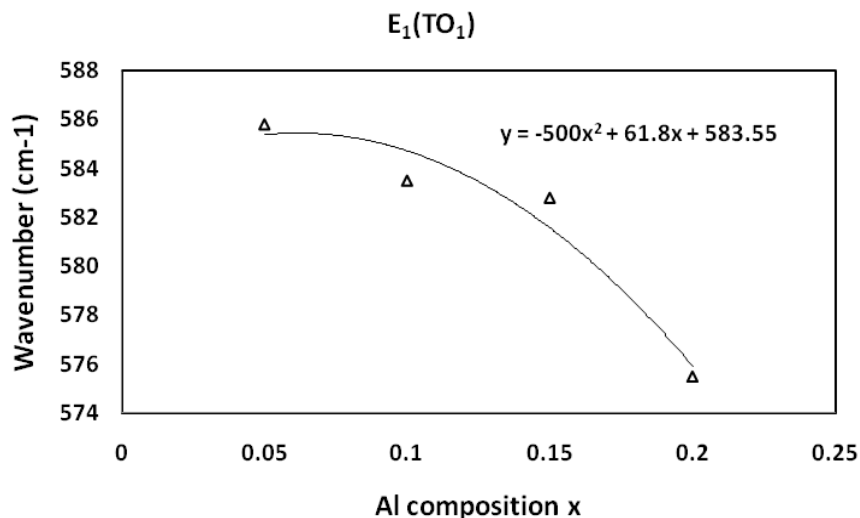


Figure 5. The $E_1(TO_1)$ optical phonon mode behaviour of $Al_xIn_yGa_{1-x-y}N$ ($0 \leq x \leq 0.2$), the solid line represents the non-linear interpolation of the $Al_xIn_yGa_{1-x-y}N$ $E_1(TO_1)$ data.

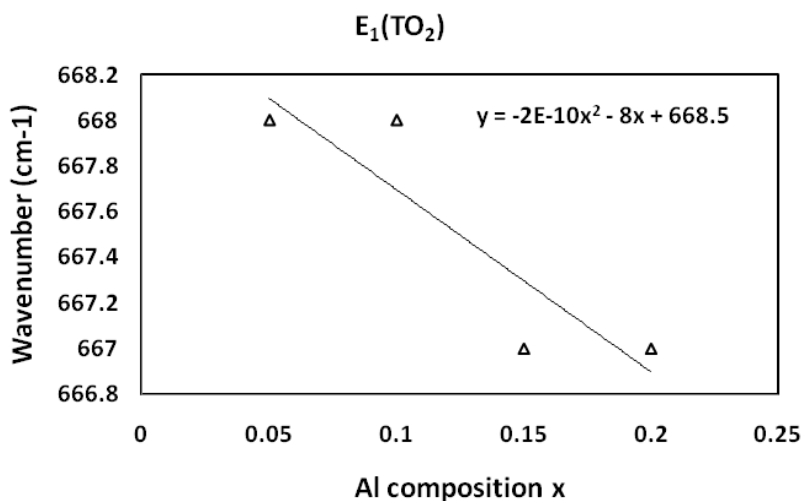


Figure 6. The $E_1(TO_2)$ optical phonon mode behaviour of $Al_xIn_yGa_{1-x-y}N$ ($0 \leq x \leq 0.2$), the solid line represents the non-linear interpolation of the $Al_xIn_yGa_{1-x-y}N$ $E_1(TO_2)$ data.

Table 1. Frequencies of optical phonon modes of $Al_xIn_yGa_{1-x-y}N$ obtained from polarized IR reflectance measurements.

Composition x (%)	$A_1(LO)$ (cm^{-1})		$E_1(TO)$ (cm^{-1})	
	$A_1(LO_1)$	$A_1(LO_2)$	$E_1(TO_1)$	$E_1(TO_2)$
0.05	801	744	585.8	668
0.10	800	745	583.5	668
0.15	801	745	582.8	667
0.20	803	746	575.5	667

For a clearer illustration of the composition dependence of the observed phonon modes of $A_1(LO_1)$, $A_1(LO_2)$, $E_1(TO_1)$ and $E_1(TO_2)$, the variations of these modes as functions of Al composition x are plotted within a composition interval of $0 \leq x \leq 0.2$. The results are shown in Figs. 3, 4, 5 and 6, respectively. As can be seen, the frequencies of $A_1(LO_1)$ and $A_1(LO_2)$ phonon modes increase with the increasing Al composition. On the other hand, the frequencies of the $E_1(LO_1)$ phonon mode decrease with increasing aluminium composition, this indicating a OM behaviour, while the frequency of the $E_1(TO)$ phonon mode exhibit TM behaviour, where two sets of modes are observed, each set corresponding to one of the pure crystals that compose the alloy, i.e., GaN and AlN.

4. CONCLUSIONS

Quaternary $Al_xIn_yGa_{1-x-y}N$ thin film alloys have been grown on c-plane sapphire substrates with a low-temperature-deposited AlN buffer layer, using PA-MBE with different aluminium (Al) mole fractions x ranging from 0.0 to 0.2 and constant indium (In) mole fraction $y = 0.1$. The alloys have been investigated using FTIR. The zone-centre optical phonons of the quaternary nitrides have also been identified. The optical phonon modes in $Al_xIn_yGa_{1-x-y}N$ exhibited two-mode behaviour. These results are in good agreement with those obtained by other groups of researchers [13, 14]. However, the frequency of these modes is relatively different because of varying mole fractions used and the different growth parameters and techniques employed.

References

1. S.N. Mohammad, A.A. Salvador, H. Morkoc, Emerging gallium nitride based devices ,Proceedings of the IEEE 83 (1995) 1306-1355.
2. S. Nakamura, *Mater. Sci. Eng. B* 50 (1997) 277-284.
3. L. Eastman, K. Chu, W. Schaff, M. Murphy, N. G. Weimann and T. Eustis: *MRS Internet J. Nitride Semicond. Res.* 2 (1997) 17-23
4. M. Shatalov, A. Chitnis, V. Adivarahan, A. Lunev, J. Zhang, J.W. Yang, Q. Fareed, G. Simin, A. Zakheim, M. Asif Khan, R. Gaska, M.S. Shur, *Appl. Phys. Lett.* 78 (2001) 817-819.
5. J.P. Zhang, V. Adivarahan, H.M.Wang, Q. Fareed, E. Kuokstis, A. Chitnis, *Japan. J. Appl. Phys.* 40 (2001) L921-L924.
6. T. Wang, Y.H. Liu, Y.B. Lee, J.P. Ao, J. Bai, S. Sakai, *Appl. Phys. Lett.* 81 (2002) 2508-2510.
7. S. Masui, Y. Matsuyama, T. Yanamoto, T. Kozaki, S. Nagahama and T. Mukai *Jpn. J. Appl. Phys.*, Vol. 42(2003) L1318-L1320.
8. Y. Liu, T. Egawa, H. Ishikawa, B. Zhang, M. Hao, *Japan. J. Appl. Phys.* Vol 43 (2004) 2414-2418.
9. V. Fiorentini, F. Bernardini, F. Della Sala, A. Di Carlo, and P. Lugli, *Phys. Rev. B* 60, (1999) 8849-8858.
10. Hirayama, H. *J. Appl. Phys.*, Vol. 97, (2005), 091101-091119.
11. Akinori Koukitu, Yoshinao Kumagai, Hisashi Seki, *J. Crystal Growth* 221 (2000) 743-750.
12. A. Kasic, M. Schubert, J. Off, F. Scholz, S. Einfeldt, D. Hommel, *Phys. Status Solidi (b)* 234 (2002) 970-974 .
13. A. Cros, A. Cantarero, N.T. Pelekanos, A. Georgakilas, J. Pomeroy, M. Kuball, *Phys. Status Solidi (b)* 243 (2006)1674-1678.
14. C.H. Chen, Y.F. Chen, Z.H. Lan, L.C. Chen, K.H. Chen, H.X. Jiang, J.Y. Lin, *Appl. Phys. Lett.* 84 (2004) 1480–1482.

15. R.S. Zheng, T. Taguchi, M. Matsuura, *Phys. Rev. B* 66 (2002) 075327-075333.
16. T. Dumelow, T.J. Parker, S.R.P. Smith, and D.R. Tilley, *Surf. Sci. Rep.* 17 (1993) 151-212.
17. H. Sobotta, H. Neumann, R. Franzheld and W. Seifert, *Phys. Stat. Sol. (b)*. 174 (1992) K57-K60.
18. C. Wetzel, E.E. Haller, H. Amano, I. Akasaki, *Appl. Phys. Lett.*, 68 (1996) 2547-2549.
19. D.W. Berreman, *Phys. Rev.* 130 (1963) 2193-2198.
20. M. Schubert, T.E. Tiwald, C.M. Herzinger, *Phys. Rev. B* 61 (2000) 8187-8201.
21. M. Kazan, P. Masri, M. Sumiya, *J. Appl. Phys.* 100 (2006) 013508-013513.